MUTATION RESEARCH-FUNDAMENTAL AND MOLECULAR MECHANISMS OF MUTAGENESIS (2004) 556 1-2:117-126.

Chromosome analysis of mouse one-cell androgenones derived from a sperm nucleus exposed to topoisomerase II inhibitors at pre- and post-fertilization stages

Tateno, H; Kamiguchi, Y

Chromosome analysis of mouse one-cell androgenones derived from a sperm nucleus exposed to topoisomerase II inhibitors at pre- and post-fertilization stages

Hiroyuki Tateno*, and Yujiroh Kamiguchi

Department of Biological Sciences, Asahikawa Medical College,

2-1 Midorigaoka-higashi, Asahikawa 078-8510, Japan.

*Correspondence to: Dr. Hiroyuki Tateno

Department of Biological Sciences, Asahikawa Medical College,

2-1 Midorigaoka-higashi, Asahikawa 078-8510, Japan.

Tel: +81-(0)166-68-2730

Fax: +81-(0)166-68-2783

E-mail: htateno@asahikawa-med.ac.jp

Abstract

Mouse spermatozoa and androgenetic one-cell embryos (androgenones) at various developmental stages were exposed to etoposide (1 μM), a topoisomerase II (topo II) poison, or to either of two catalytic inhibitors: ICRF-193 (10 μM) or merbarone (50 μM), for 2 h in order to study the clastogenic effects of these drugs on remodeled sperm chromatin. None of the drugs induced structural chromosome aberrations in condensed chromatin of spermatozoa. However, etoposide and merbarone exerted strong clastogenic actions on remodeled chromatin of androgenones. Expanding chromatin was most sensitive to both of these drugs at the time of pronuclear formation, as nearly 100 % of androgenones exposed at this stage displayed structural chromosome aberrations. ICRF-193 did not affect sperm chromatin at all remodeling stages. A majority of the aberrations induced by etoposide and merbarone were of the chromosome type. Chromosome exchanges, including translocation, dicentric, and ring chromosomes, preferentially appeared following exposure at the early stages of chromatin remodeling. Thus, despite their different modes of topo II inhibition, etoposide and merbarone showed similar clastogenic actions on remodeled sperm chromatin. These results suggest that the formation of transient DNA cleavage, mediated by ooplasmic topo II, accompanies the remodeling. The present findings provide insight into the mechanisms by which structural aberrations are generated in paternal chromosomes.

Key words: topoisomerase II inhibitors, sperm chromatin remodeling, chromosome aberrations, androgenones,

1. Introduction

In eukaryotic cells, type II topoisomerases (topo II) mediate chromosome condensation and segregation in the M phase and help maintain the structure of metaphase chromosomes [1−3]. Thus, the inhibition of topo II activity potentially causes aneuploidy and structural chromosome aberrations in dividing cells [4]. Mammalian oocytes and spermatocytes during meiotic divisions cannot escape from chromosome damage induced by topo II inhibitors such as etoposide, bisdioxopiperazine ICRF-193 and merbarone. Etoposide belongs to a class of topo II poisons that stabilize enzyme-DNA cleavable complexes [5]. ICRF-193 and merbarone belong to another class of topo II inhibitors, referred to as catalytic inhibitors [6, 7]. When murine primary and secondary oocytes were exposed to etoposide, both aneuploidy and structural chromosome aberrations were frequently induced [8−11]. ICRF-193 was also clastogenic and aneugenic to mouse secondary oocytes [12]. Etoposide's ability to induce structural chromosome aberrations and aneuploidy in male meiosis has been reported in mice [13−16] and rats [17]. Furthermore, merbarone has been shown to be aneugenic to mouse spermatocytes [16, 18].

On the other hand, there is no available information on the cytogenetic effects of topo II inhibitors on sperm nuclei at pre- or post-fertilization stages, except that mouse testicular sperm nuclei did not suffer chromosome damage by etoposide [11, 15]. Sperm nuclei exhibit chromatin dynamics with fertilization as a turning point [19−21]. Before fertilization, mature sperm nuclei are highly condensed, but during

fertilization they decondense and extensively expand to form enlarged male pronuclei. An immunocytological study in the mouse revealed that mature sperm nuclei had no topo II, while decondensing sperm nuclei showed a distribution of topo II originating from ooplasmic stores [22]. Interestingly, it has been reported that teniposide, a topo II poison, induced endogenous DNA nicks in decondensing mouse sperm nuclei during fertilization [23]. These results suggest that ooplasmic topo II is involved in molecular remodeling of sperm chromatin. Hence the inhibition of ooplasmic topo II during fertilization may cause structural aberrations in paternal chromosomes.

To confirm the probability of this, mouse sperm nuclei at pre- and post-fertilization stages were exposed to etoposide, ICRF-193 and merbarone, and their chromosomes were identified as male pronuclear chromosomes in eggs at the first cleavage metaphase. Previous studies found that etoposide and ICRF-193 can induce chromosome aberrations in mouse oocytes during meiosis II [9, 12]. In addition, our preliminary experiment with mouse parthenogenetic embryos showed that merbarone had clastogenic action on secondary oocytes. To evaluate clastogenic effect of the inhibitors on sperm nuclei, male pronuclear chromosomes should be discriminated from female pronuclear chromosomes. Usually, male pronuclear chromosomes appear longer and less condensed than female pronuclear chromosomes. However, our experience shows that this does not always a reliable indication of male pronuclear chromosomes in mouse zygotes arrested at metaphase by mitotic inhibitors.

In the present study, therefore, androgenetic embryos (androgenones) were microsurgically produced by injecting sperm nuclei into enucleated

oocytes to makes sure that we look only at sperm-derived chromosomes.

2. Materials and Methods

2.1. Topo II inhibitors

Etoposide (CAS No. 33419-42-0) and ICRF-193 were purchased from Sigma-Aldrich (St. Louis, MO, USA) and Funakoshi (Tokyo, Japan), respectively. Merbarone was supplied by the Developmental Therapeutic Program, National Cancer Institute, Bethesda, MD, USA. Dimethyl sulfoxide (DMSO) was used as a solvent to dissolve etoposide at a concentration of 1 mM, ICRF-193 at a concentration of 10 mM, and merbarone at a concentration of 50 mM. These solutions were divided into 5 µl aliquots and stored at −80 °C until approximately 2 h before use. The stock of etoposide, ICRF-193, and merbarone were diluted with the appropriate medium to make 1 µM, 10 µM, and 50 µM concentrations, respectively. Etoposide and merbarone at their respective *in vitro* concentrations cause structural chromosome aberrations in 80−100 % of mouse secondary oocytes (unpublished data), and ICRF-193 at 10 µM *in vitro* causes structural chromosome aberrations in more than 50 % of mouse secondary oocytes [12]. The final DMSO concentration in each chemical treatment was 0.1 %.

2.2. Media

TYH medium was used for incubating spermatozoa under 5 % CO_2 in air [24]. The medium for handling spermatozoa under 100 % air was a modified TYH containing 20 mM Hepes-Na, a reduced amount of $NaHCO_3$ (5 mM), and 0.1 mg/ml polyvinyl alcohol (PVA: cold water soluble, Sigma-Aldrich) in place of bovine serum albumin. This was referred to as Hepes-TYH medium. The medium used for culturing oocytes and androgenones under 5 % CO_2 in air was CZB [25] supplemented with 5.56 mM D-glucose. The medium for oocyte collection and microsurgery was a modified CZB containing 20 mM Hepes-Na, 5 mM $NaHCO_3$, and 0.1 mg/ml PVA, referred to as Hepes-CZB medium. The pH of both Hepes-TYH and Hepes-CZB media was adjusted to approximately 7.4 by the addition of 1 N HCl.

2.3. Production of androgenones

B6D2F1 hybrid female mice 7−12 weeks of age were superovulated by an intraperitoneal injection of 8−10 IU pregnant mare's serum gonadotropin (PMSG) followed 48 h later with an injection of 8−10 IU human chorionic gonadotropin (hCG). Oocytes at metaphase II were collected from the oviducts between 14 and 15 h after hCG injection and freed from cumulus cells by treatment with 0.1 % testicular hyaluronidase in Hepes-CZB medium for 3−5 min at room temperature (24−25 °C). The cumulus-free oocytes were temporarily kept in CZB medium at 37 °C and then transferred into a droplet (10 µl) of Hepes-CZB medium containing 5 µg/ml cytochalasin B (Sigma-Aldrich) and enucleated as described elsewhere [26]. The enucleation

was performed at room temperature. The enucleated oocytes were thoroughly washed with CZB medium and kept in the medium at 37 °C until use.

Mature spermatozoa were collected from the cauda epididymides of B6D2F1 male mice 7−12 weeks of age, and were incubated in TYH medium for 1.5−2.0 h at 37 °C. The motile spermatozoa were transferred into a droplet (10 µl) of Hepes-TYH medium containing 10 % (w/v) polyvinylpyrrolidone (PVP: Nacalai Tesque, Kyoto, Japan). Sperm heads were separated from the tail by applying one or more piezo pulses; the sperm heads were then individually injected into enucleated oocytes by the intracytoplasmic sperm injection (ICSI) technique established by Kimura and Yanagimachi [27]. The ICSI procedure was performed in a droplet (10 µl) of Hepes-CZB medium at room temperature. In every microsurgery, 9−25 oocytes were used and sperm injection was finished within 30 min. Sperm-injected eggs (androgenones) were cultured in a droplet (100 µl) of CZB medium under paraffin oil at 37 °C.

2.4. Sperm nuclear remodeling in enucleated eggs

Cytological preparations of several androgenones were made 1, 2, 3, 4, 6, and 8 h after ICSI as follows. Zonae pellucidae were removed by digestion with 0.5 % protease (Kaken Pharmaceuticals, Tokyo) in Ca^{2+}/Mg^{2+}-free Dulbecco's phosphate buffered saline (PBS). The androgenones were washed once with CZB, and fixed and air-dried according to Mikamo and Kamiguchi [28]. The slides were conventionally stained with 2 % Giemsa (Merck Japan, Tokyo) for 8 min. DNA synthesis was analyzed using BrdU labeling and detection kit (Roche, Mannheim, Germany). In brief, androgenones were

cultured in CZB supplemented with 10 μM BrdU at 37 °C. They were fixed in 10 % neutralized formalin at 3, 4, 5, or 6 hr after ICSI, kept overnight at 4 °C, and then washed with PBS containing 0.3 % bovine serum albumin (PBS/BSA). The DNA was denatured in 2N HCl for 1 h at 37 °C. The androgenones were neutralized by borate buffer (pH 8.5) for 15 min at room temperature. After being thoroughly washed with PBS/BSA, the androgenones were incubated in PBS/BSA containing anti-BrdU antibody for 45 min at 37 °C. They were washed one time with PBS/BSA, incubated in PBS/BSA containing fluorescent anti-mouse IgG for 45 min at 37 °C, and then kept in PBS/BSA overnight at 4 °C to wash out excess IgG. The androgenones were placed on poly-L-lysine coated glass slides and covered with Vectashield mounting medium (Vector, Burlingame, CA) for fluorescent microscopy.

2.5. Chemical treatments

On the basis of the results obtained in the preliminary analysis of sperm nuclear development, the following stages were determined as targets of the topo II inhibitors.

(1) condensed chromatin of spermatozoa just before ICSI

(2) decondensing and recondensing chromatin in androgenones 0 to 2 h after ICSI

(3) expanding chromatin at the time of pronuclear formation in androgenones 2 to 4 h after ICSI

(4) pronuclei at G_1 to early S phases in androgenones 4 to 6 h after ICSI

(5) pronuclei at S phase in androgenones 6 to 8 h after ICSI

When condensed chromatin was exposed to topo II inhibitors, spermatozoa were incubated in TYH medium containing topo II inhibitors for 2 h. Then they were washed with Hepes-TYH medium by centrifugation and prepared for ICSI. When remodeled chromatin was exposed to topo II inhibitors, androgenones were transferred, at a predetermined time, to CZB medium containing topo II inhibitors and incubated for 2 h. After being fully washed with CZB medium, the androgenones were further cultured in the medium at 37 °C.

2.6. Chromosome preparations and analysis

Six to eight hours after ICSI, androgenones were transferred to CZB medium containing 0.02 μg/ml vinblastine sulfate (Sigma-Aldrich) and cultured until they reached the first cleavage metaphase. Between 18 and 20 h after ICSI, androgenones were treated with 0.5 % protease to loosen the zona pellucida and exposed to a hypotonic solution (1:1 mixture of 1 % sodium citrate and 30 % fetal bovine serum) for 10 min at room temperature. Chromosome slides of androgenones were made by the gradual-fixation/air-drying method [28]. The chromosome slides were stained with 2 % Giemsa for 8 min for conventional chromosome analysis. Subsequently, each chromosome was C-banded to stain the constitutive heterochromatin, as previously described [29]. All autosomes and an X chromosome of B6D2F1 mice used in this study have a positive C-band at the centromeric region and the whole Y chromosome shows intermediate C-band

staining. According to standard aberration scoring, a case with 20 centric chromosomes and an excess acentric fragment was classified as a break. While an achromatic lesion was classified as a gap, and a chromosome with two positive C-bands and a derivative acentric fragment was considered a dicentric aberration. Both a chromosome with an interstitially positive C-band and an extremely long centric chromosome were translocations. Because it was impossible to perfectly detect reciprocal translocations by C-banding analysis, underestimation of this aberration type was unavoidable.

2.7. Statistical analysis

Differences between the treated and untreated groups in the percentage of androgenones with structural chromosome aberrations were compared using the chi-square test. Either the chi-square test or Fisher's exact probability test was used to compare the ratio of each aberration type. Individual group comparisons of frequencies of structural chromosome aberrations per cell were performed by the one-factor ANOVA and Bonferroni/Dunn post-hoc tests. Differences were considered significant at $P < 0.05$.

3. Results

3.1. Nuclear remodeling in androgenones

Figure 1 shows the development of mouse sperm nuclei injected into enucleated oocytes. At 1 h after ICSI, sperm nuclei were decondensed and swollen about two-fold with trace of their original form. At 2 h, decondensed nuclei were recondensed. They looked like a small chromatin mass. At 3 h, chromatin dispersed again and formed a small pronucleus. At 4 h or later, well-developed pronuclei were always seen. However, no incorporation of BrdU was detected in eight androgenones examined at 4 h. At 5 h, two of 12 androgenones incorporated BrdU, and at 6 h six of 11 pronuclei underwent DNA synthesis. Thus, there was no a marked change in sperm chromatin dynamics and timing of DNA synthesis in enucleated eggs.

3.2. Chromosome analysis

Table 1 summarizes the results of the chromosome analysis at the first cleavage metaphase of the androgenones derived from sperm chromatin exposed to each of the three topo II inhibitors at the pre- and post-fertilization stages. ICRF-193 yielded no significant increase in structural chromosome aberrations in sperm chromatin at any stage. Etoposide and merbarone induced no structural chromosome aberrations in condensed sperm chromatin at the pre-fertilization stage. Alternatively, both chemicals caused severe damage in sperm chromatin at every post-fertilization stage. Expanding chromatin at the time of pronuclear formation in androgenones was most sensitive to both etoposide and merbarone, at 2 to 4 h after ICSI, as nearly 100 % of androgenones exposed to these chemicals in this stage displayed multiple structural chromosome

aberrations (Fig. 2). In both chemical groups, the frequency of aberrant chromosomes per cell exceeded 5 (Fig. 3). Based on the percentage of chromosomally abnormal androgenones and the frequency of aberrant chromosomes per cell, the next most sensitive stage was 4 to 6 h after ICSI (pronucleus at G_1 to early S phases) in the etoposide group (86.3 % and 1.99), and 0 to 2 h after ICSI (decondensation and recondensation phases) in the merbarone group (93.5 % and 3.32).

Most of the aberrations caused by etoposide and merbarone were of the chromosome type (Fig. 4). In androgenones exposed to these chemicals 0 to 2 h after ICSI (decondensation and recondensation phases), 54.9 % of aberrations in the etoposide group were chromosome exchanges including dicentric, translocation, or ring types, and 48.7 % of aberrations in the merbarone group were these exchange types. However, the percentage of chromosome exchanges was significantly reduced after exposure at subsequent stages ($P < 0.05–0.0001$, χ^2-test). In both chemical groups, the incidence of chromatid exchanges was evidently high following exposure in the S phase (6 to 8 h after ICSI) compared to other exposure groups ($P <$ 0.0001, Fisher's exact probability test). Overall, the types and frequencies of structural chromosome aberrations induced by 1 μM etoposide were similar to those induced by 50 μM merbarone.

4. Discussion

The present study revealed that the cytogenetic effects of topo II inhibitors on sperm chromatin differed considerably depending on the type of inhibitors and the remodeled states of chromatin at the time of exposure.

ICRF-193 caused no cytogenetic damage to sperm chromatin at any developmental stage. Despite the different modes of topo II inhibition, etoposide and merbarone had similar clastogenic profiles with sperm chromatin: neither of them affected the condensed chromatin of mature spermatozoa, but both induced severe damage in sperm chromatin during fertilization, particularly during the extensive expansion of the sperm chromatin at the time of pronucleus formation. Furthermore, chromosome aberrations induced by etoposide and merbarone were mostly of chromosome-type, and chromosome exchanges frequently occurred in androgenones exposed to these drugs 0−2 h after ICSI. These findings indicate that DNA double strand breaks are produced by etoposide or merbarone exposure and the DNA breaks at the early stages of chromatin remodeling can be repaired potentially by ooplasmic machinery.

Jacquet et al. [30] and Matsuda et al. [31] reported that the stage of highest X-ray sensitivity in mouse fertilized eggs was the pronuclear formation stage, followed by fertilization stage and DNA synthesis stage, in this order. Most of chromosome aberrations in male genomes induced by the irradiation at pre-DNA synthesis were of chromosome-type, and the frequency of chromosome exchanges drastically decreased after the completion of pronuclear formation [31]. Thus, it is noteworthy that the present results obtained by the exposure of androgenones to etoposide and merbarone somewhat agree with the previous results obtained by X-irradiation to fertilized eggs, although the primary target differs.

There are two possible explanations for the insensitivity of condensed sperm chromatin to etoposide and merbarone. One is that these inhibitors

are not accessible to the tightly packed sperm nucleus. Another is that mature spermatozoa lack etoposide and merbarone targets. The latter has been suggested by the immunocytological findings that mature sperm nuclei lack topo II [22]. The issue may be settled by investigating whether sperm chromatin would be affected by these inhibitors when the content of disulfide bonds in protamines was reduced by dithiothreitol. The immunostaining also found that decondensing sperm nuclei distribute antibodies which recognize both isoforms (α and ß) of ooplasmic topo II [22]. The distribution of ooplasmic topo II on decondensing sperm chromatin suggests that the remodeling of sperm chromatin is accompanied by the formation of transient DNA cleavages mediated by ooplasmic topo II. Etoposide is a topo II poison that stabilizes enzyme-DNA cleavable complexes leading to DNA strand breaks [5]. This is understood as the mechanism underlying etoposide's clastogenicity.

On the other hand, merbarone is classified as a catalytic inhibitor that blocks topo II-mediated DNA strand breaks without stabilizing cleavable complexes [6]. In support of this, other studies have shown that there was no increase in DNA strand breaks in cultured mammalian somatic cells treated with merbarone [32, 33]. Furthermore, merbarone exclusively induced aneuploidy during male meiotic divisions in mice [16, 18]. Based on these findings, merbarone has been considered an aneugen not a clastogen. Recently, however, micronucleus assays using human cultured somatic cells and mouse bone marrow cells have demonstrated that merbarone can induce both structural chromosome aberrations and aneuploidy [34, 35]. Although the molecular mechanisms underlying the clastogenicity of merbarone

remain to be fully elucidated, the dysfunction of ooplasmic topo II by this agent may cause the torsional stress of DNA to accumulate in remodeled sperm chromatin, thereby generating DNA strand breaks. In the present results, expanding chromatin of androgenones at 2−4 h after ICSI was extremely sensitive to merbarone, as compared to that of other groups. At this time, in succession to the replacement of protamines by histones, DNA strands rapidly and maximally expand for the subsequent pronuclear DNA synthesis [20]. Therefore, there is more opportunity for DNA to be subject to breaks from torsional forces.

In spite of sperm chromatin states, the treatment with 1 μM etoposide or 50 μM merbarone for 2 h at post-fertilization stages affected more than 50 % of androgenones. Unfortunately, no comparable data on *in vitro* sensitivity of other germ cell stages to these topo II inhibitors has been reported. However, when human G_0 lymphocytes were exposed *in vitro* to 50 μM etoposide for 2 h, only 4 % of treated cells had unstable chromosome aberrations [36]. When human epidermoid cancer KB cells were treated *in vitro* with 1.25 μM etoposide for 6 h, the frequency of chromosomally aberrant cells was about 42 % [37]. Although comparable data on *in vitro* sensitivity of somatic cells has been limited to etoposide, sperm DNA during chromatin remodeling seems to be more vulnerable to topo II inhibitors than somatic DNA.

In contrast to merbarone, another catalytic inhibitor, ICRF-193, was not clastogenic to mouse sperm chromatin during remodeling. The difference in clastogenicity between merbarone and ICRF-193 may depend on their respective molecular modes of action to topo II. Merbarone primarily blocks

topo II-mediated DNA strand breaks, thus forming pre-cleavable complexes, while ICRF-193 is believed to stabilize the closed clamp form of topo II by creating post-passage complexes [7]. Supposing that DNA torsional stress can be relieved by post-passage complexes, the generation of DNA strand breaks may be circumvented even in the presence of ICRF-193. However, ICRF-193 and the related compounds should be recognized as clastogenic to mitotic cells [38−40] and female meiotic cells [12], although the mechanisms are poorly understood.

The present findings afford two other insights into the mechanisms by which structural aberrations are generated in paternal chromosomes. One mechanism is the structural and biochemical alteration of sperm chromatin. When topo II is incapable of acting on the altered sperm chromatin, DNA strand breaks may be generated as occurs when inhibitors inactivate ooplasmic topo II. This idea is supported by our previous findings that severe structural chromosome aberrations were induced in mouse spermatozoa following treatment with ethanol [41] or demembranation by sonication [29]. The other mechanism is the delay in the remodeling of sperm chromatin behind the meiotic progression of secondary oocytes. In general, the level of topo II (α isoform) shows cell-cycle dependency; it is relatively low in G_1/S phases and high in G_2/M phases [3]. Unless sperm chromatin was adequately and timely exposed to ooplasmic topo II at the M phase, the torsional stress on DNA during chromatin remodeling would not be relieved completely, leading to strand breaks. This may explain why structural aberrations were significantly induced in paternal chromosomes when sperm nuclear development was delayed behind egg development in cross-fertilization

between Chinese hamster spermatozoa and Syrian hamster oocytes [42, 43], and it may explain the significant increase of structural aberrations in paternal chromosomes of mouse embryos produced by delayed sperm injection into parthenogenetic eggs [44].

Some of topo II inhibitors are clinically used as antineoplastic drugs. In addition, some agricultural, industrial and pharmaceutical chemicals may potentially interact with topo II. Further investigation should be pursued to evaluate the cytogenetic risk of topo II inhibitors on mammalian gametes as well as to understand the mechanism underlying the chromosomal mutagenicity of topo II inhibitors.

Acknowledgments

The authors thank Dr. Robert J. Schultz of the National Cancer Institute (Drug Synthesis & Chemistry Branch) for kindly providing merbarone. This study was supported by The Tutikawa Memorial Fund for Study in Mammalian Mutagenicity (H.T.).

References

[1] J.L. Nitiss, Investigating the biological functions of DNA topoisomerases in eukaryotic cells, Biochem. Biophys. Acta 1400 (1998) 63-81.

[2] J.C. Wang, Cellular roles of DNA topoisomerases: a molecular perspective, Nat. Rev. Mol. Cell Biol. 3 (2002) 430-440.

[3] F. Cortés, N. Pastor, S. Mateos, I. Domíngues, Roles of DNA topoisomerases in chromosome segregation and mitosis, Mutat. Res. 543 (2003) 59-66.

[4] R.D. Anderson, N.A. Berger, Mutagenicity and carcinogenicity of topoisomerase-interactive agents, Mutat. Res. 309 (1994) 109-142.

[5] D.A. Burden, N. Osheroff, Mechanism of action of eukaryotic topoisomerase II and drugs targeted to the enzyme, Biochem. Biophys. Acta 1400 (1998) 139-154.

[6] J.M. Fortune, N. Osheroff, Merbarone inhibits the catalytic activity of human topoisomerase IIα by blocking DNA cleavage, J. Biol. Chem. 273 (1998) 17643-17650.

[7] T. Ando, R. Ishida, Catalytic inhibitors of DNA topoisomerase II, Biochem. Biophys. Acta 1400 (1998) 155-171.

[8] J.B. Mailhes, F. Marchetti, G.L. Phillips Jr, D.R. Barnhill, Preferential pericentric lesions and aneuploidy induced in mouse oocytes by the topoisomerase II inhibitor etoposide, Teratogen. Carcinogen. Mutagen. 14 (1994) 39-51.

[9] J.B. Mailhes, F. Marchetti, D. Young, S.N. London, Numerical and structural chromosome aberrations induced by etoposide (VP16) during

oocyte maturation of mice: transmission to one-cell zygotes and damage to dictyate oocytes, Mutagenesis 11 (1996) 357-361.

[10] H. Tateno, Y. Kamiguchi, Meiotic stage-dependent induction of chromosome aberrations in Chinese hamster primary oocytes exposed to topoisomerase II inhibitor etoposide, Mutat. Res. 476 (2001) 139-148.

[11] F. Marchetti, J.B. Bishop, L. Cosentino, D. Moor II, A.J. Wyrobek, Paternally transmitted chromosomal aberrations in mouse zygotes determine their embryonic fate, Biol. Reprod. 70 (2004) 616-624.

[12] H. Tateno, Y. Kamiguchi, Abnormal chromosome migration and chromosome aberrations in mouse oocytes during meiosis II in the presence of topoisomerase II inhibitor ICRF-193, Mutat. Res. 502 (2002) 1-9.

[13] M. Kallio, J. Lähdetie, Analysis of micronuclei induced in mouse early spermatids by mitomycin C, vinblastine sulfate or etoposide using fluorescence *in situ* hybridization, Mutagenesis 8 (1993) 561-567.

[14] M. Kallio, J. Lähdetie, Fragmentation of centromeric DNA and prevention of homologous chromosome separation in male mouse meiosis *in vivo* by the topoisomerase II inhibitor etoposide, Mutagenesis 11 (1996) 435-443.

[15] F. Marchetti, J.B. Bishop, X. Lowe, W.M. Generoso, J. Hozier, A.J. Wyrobek, Etoposide induces heritable chromosomal aberrations and aneuploidy during male meiosis in the mouse, Proc. Natl. Acad. Sci. U.S.A. 98 (2001) 3952-3957.

[16] S.M. Attia, T.E. Schmid, O.A. Badary, F.M. Hamada, I.-D. Adler, Molecular cytogenetic analysis in mouse sperm of chemically induced

aneuploidy: studies with topoisomerase II inhibitors, Mutat. Res. 520 (2002) 1-13.

[17] J. Lähdetie, A. Keiski, A. Suutari, J. Toppari, Etoposide (VP-16) is a potent inducer of micronuclei in male rat meiosis: spermatid micronucleus test and DNA flow cytometry after etoposide treatment, Environ. Mol. Mutagen. 24 (1994) 192-202.

[18] M. Kallio, J. Lähdetie, Effects of the DNA topoisomerase II inhibitor merbarone in male mouse meiotic divisions in vivo: cell cycle arrest and induction of aneuploidy, Environ. Mol. Mutagen. 29 (1997) 16-27.

[19] P.G. Adenot, M.S.Szöllösi, M. Geze, J-P. Renard, P. Debey, Dynamics of paternal chromatin changes in live one-cell mouse embryo after natural fertilization, Mol. Reprod. Dev. 28 (1991) 23-34.

[20] S.D. Perreault, Chromatin remodeling in mammalian zygotes, Mutat. Res. 296 (1992) 43-55.

[21] D.W. McLay, H.J. Clarke, Remodeling the paternal chromatin at fertilization in mammals, Reproduction 125 (2003) 625-633.

[22] J, St. Pierre, D.J. Wright, T.C. Rowe, S.J. Wright, DNA topoisomerase II distribution in mouse preimplantation embryos, Mol. Reprod. Dev. 61 (2002) 335-346.

[23] D. Bizzaro, G. Manicardi, P.G. Bianchi, D. Sakkas, Sperm decondensation during fertilisation in the mouse: presence of DNase I hypersensitive sites *in situ* and a putative role for topoisomerase II, Zygote 8 (2000) 197-202.

[24] Y. Toyoda, M. Yokoyama, T. Hoshi, Studies on the fertilization of mouse eggs in vitro. I. In vitro fertilization of mouse eggs by fresh epididymal

semen, Jpn. J. Anim. Reprod. 16 (1971) 147-151.

[25] C.L. Chatot, A. Ziomek, B.D. Bavister, J.L. Lewis, I. Torres, An improved culture medium supports development of random-bred 1-cell mouse embryos *in vitro*, J. Reprod. Fert. 86 (1989) 679-688.

[26] T. Wakayama, A.C.F. Perry, M. Zuccotti, K.R. Johnson, R. Yanagimachi, Full-term development of mice from enucleated oocytes injected with cumulus cell nuclei, Nature 394 (1998) 369-374.

[27] Y. Kimura, R. Yanagimachi, Intracytoplasmic sperm injection in the mouse, Biol. Reprod. 52 (1995) 709-720.

[28] K. Mikamo, Y. Kamiguchi, A new assessment system for chromosomal mutagenicity using oocytes and early zygotes of the Chinese hamster, in: T. Ishihara, M.S. Sasaki (Eds.), Radiation-induced chromosome damage in man, New York, Alan R. Liss, 1983, pp. 411-432.

[29] H. Tateno, Y. Kimura, R. Yanagimachi, Sonication per se is not as deleterious to sperm chromosomes as previously inferred, Biol. Reprod. 63 (2000) 341-346.

[30] P. Jacquet, G. Kervyn, G.De Clercq, Studies in vitro on mouse-egg radiosensitivity from fertilization up to the first cleavage, Mutat. Res. 110 (1983) 351-365.

[31] Y. Matsuda, N. Seki, T. Utsugi-Takeuchi, I. Tobari, Changes in X-ray sensitivity of mouse eggs from fertilization to the early pronuclear stage, and their repair capacity, Int. J. Radiat. Biol. 55 (1989) 233-256.

[32] F.H. Drake, G.A. Hofmann, S.M. Mong, J.O. Bartus, R.P. Hertzberg, R.K. Johnson, M.R. Mattern, C.K. Mirabelli, In vitro and intracellular inhibition of topoisomerase II by the antitumor agent merbarone,

Cancer Res. 15 (1989) 2578-2583.

[33] M. Chen, W.T. Beck, Differences in inhibition of chromosome separation and G_2 arrest by DNA topoisomerase II inhibitors merbarone and VM-26, Cancer Res. 55 (1995) 1509-1516.

[34] L. Wang, D.A. Eastmond, Catalytic inhibitors of topoisomerase II are DNA damaging agents: induction of chromosomal damage by merbarone and ICRF-187, Environ. Mol. Mutagen. 39 (2002) 348-356.

[35] S.M. Attia, U. Kliesch, G. Schriever-Schwemmer, O.A. Badary, F.M. Hamada, I.-D. Adler, Etoposide and merbarone are clastogenic and aneugenic in the mouse bone marrow micronucleus test complemented by fluorescence in situ hybridization with the mouse *minor* satellite DNA probe, Environ. Mol. Mutagen. 41 (2003) 99-103.

[36] P. Mosesso, F. Darroudi, M. van den Berg, S. Vermeulen, F. Palitti, A.T. Natarajan, Induction of chromosomal aberrations (unstable and stable) by inhibitors of topoisomerase II, m-AMSA and VP-16, using conventional Giemsa staining and chromosome painting techniques, Mutagenesis 13 (1998), 39-43.

[37] H. Suzuki, Y. Tarumoto, M. Ohsawa, Topoisomerase II inhibitors fail to induce chromosome-type aberrations in etoposide-resistant cells: evidence for essential contribution of the cleavable complex formation to the induction of chromosome-type aberrations, Mutagenesis 12 (1997), 29-33.

[38] T. Ikushima, Y. Shima, Y. Ishii, Effects of an inhibitor of topoisomerase II, ICRF-193 on the formation of ultraviolet-induced chromosomal aberrations, Mutat. Res. 404 (1998) 35-38.

[39] N. Pastor, I. Domínguez, S. Mateos, F. Cortés, A comparative study of genotoxic effects of anti-topoisomerase II drugs ICRF-193 and bufalin in Chinese hamster ovary cells, Mutat. Res. 515 (2002) 171-180.

[40] N. Hajji, N. Pastor, S. Mateos, I. Domínguez, F. Cortés, DNA strand breaks induced the anti-topoisomerase II bis-dioxopiperazine ICRF-193, Mutat. Res. 530 (2003) 35-46.

[41] H. Tateno, T. Wakayama, W.S. Ward, R. Yanagimachi, Can alcohol retain the reproductive and genetic potential of sperm nuclei? Chromosome analysis of mouse spermatozoa stored in alcohol, Zygote 6 (1998) 233-238.

[42] H. Tateno, Y. Kamiguchi, Improvement of male pronuclear formation during cross-fertilization between Chinese hamster spermatozoa and Syrian hamster oocytes by nocodazole, and chromosome analysis of hybrid zygotes, Mol. Reprod. Dev. 52 (1999) 117-124.

[43] H. Tateno, Y. Kamiguchi, Dithiothreitol induces sperm nuclear decondensation and protects against chromosome damage during male pronuclear formation in hybrid zygotes between Chinese hamster spermatozoa and Syrian hamster oocytes, Zygote 7 (1999) 321-327.

[44] H. Tateno, Y. Kamiguchi, How long do parthenogenetically activated mouse oocytes maintain the ability to accept sperm nuclei as a genetic partner?, J. Assist. Reprod. Genet, (in press).

Figure legends

Figure 1

Development of mouse sperm nuclei injected into enucleated oocytes. (A) sperm head just before fertilization, (B) decondensing sperm chromatin at 1 h after ICSI, (C) recondensing sperm chromatin at 2 h after ICSI, (D) expanding sperm chromatin in a developing pronucleus at 3 h after ICSI, (E) extensively expanded sperm chromatin in an early pronucleus at 4 h after ICSI, (F) an androgenone with a well-developed pronucleus at 6 h after ICSI, (G) DNA synthesis detected by immunolabeling the incorporation of BrdU at 6 h after ICSI. Bar: 10 μm

Figure 2

Structural chromosome aberrations in an androgenone exposed to etoposide between 2 and 4 h after ICSI. There are twenty C band-positive centromeric heterochromatin spots. Two thick arrows indicate pericentric break, a short arrow an interstitial break and a long arrow a dicentric chromosome. Four derivative acentric fragments (arrowheads) are seen.

Figure 3

Frequencies of aberrant chromosomes per cell in androgenones derived from sperm chromatin exposed to etoposide (A), ICRF-193 (B) and merbarone (C) at pre- and post-fertilization stages. Frequencies with different lower cases at top of column show statistical significance ($P < 0.002$, post-hoc test).

Figure 4

Rate of different types of structural chromosome aberrations found in androgenones derived from sperm chromatin exposed to etoposide (A) and merbarone (B) at various times after ICSI (black box: chromosome break/gap; dotted box: chromosome exchange; slashed box: chromatid break/gap; white box: chromatid exchange).

Table 1. Chromosome analysis at the first cleavage metaphase of androgenones derived from sperm nuclei exposed to three different topo II inhibitors at pre- and post-fertilization stages

Chemicals (conc.)	Time of exposure	No. of cells analyzed	No.(%) of cells with structural chromosome aberrations	No. of aberrant chromosomes								
				Chromosome type					Chromatid type			Total
				break	gap	dicentric	trans-location	ring	break	gap	exchange	
None	-	163	15 (9.2)[a]	5	9	1	0	0	0	2	0	17
Etoposide	2 h before ICSI	114	13 (11.4)	5	9	0	0	0	0	0	1	15
(1 μM)	0-2 h after ICSI	116	77 (66.4)[b]	55	2	55	11	12	7	0	0	142
	2-4 h after ICSI	111	110 (99.1)[b]	430	8	121	39	14	36	0	4	652
	4-6 h after ICSI	117	101 (86.3)[b]	170	7	22	9	6	16	0	3	233
	6-8 h after ICSI	108	71 (65.7)[b]	96	4	2	3	1	13	0	24	143
ICRF-193	2 h before ICSI	101	7 (6.9)	4	2	2	0	0	0	0	0	8
(10 μM)	0-2 h after ICSI	108	10 (9.3)	5	4	4	1	0	1	0	0	15
	2-4 h after ICSI	115	14 (12.2)	10	4	0	0	0	2	1	0	17
	4-6 h after ICSI	109	7 (6.4)	3	7	1	0	0	1	0	0	12
	6-8 h after ICSI	112	10 (8.9)	4	4	0	0	0	1	0	1	10
Merbarone	2 h before ICSI	113	10 (8.8)	1	8	0	0	0	0	0	1	10
(50 μM)	0-2 h after ICSI	107	100 (93.5)[b]	144	3	151	9	13	35	0	0	355
	2-4 h after ICSI	105	103 (98.1)[b]	363	9	107	16	13	25	1	7	541
	4-6 h after ICSI	112	75 (67.0)[b]	104	7	13	1	3	2	0	2	132
	6-8 h after ICSI	110	62 (56.4)[b]	75	3	4	1	1	5	0	22	111

a-b: $P < 0.0001$

Figure 1

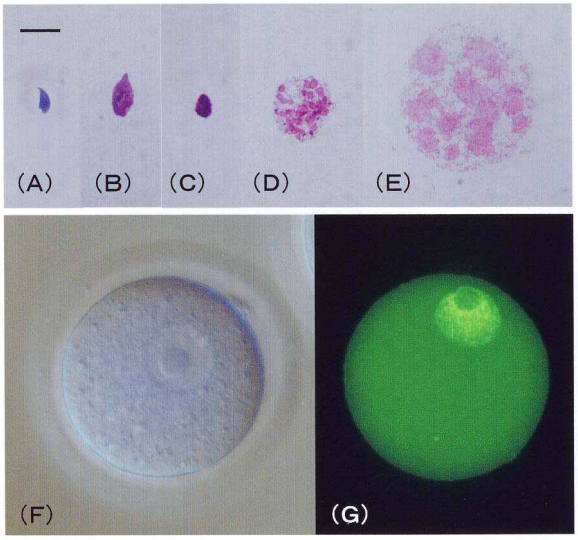

Figure 2

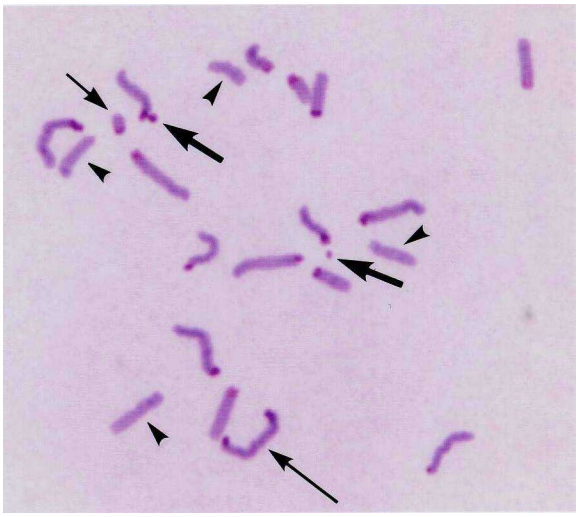

Figure 3

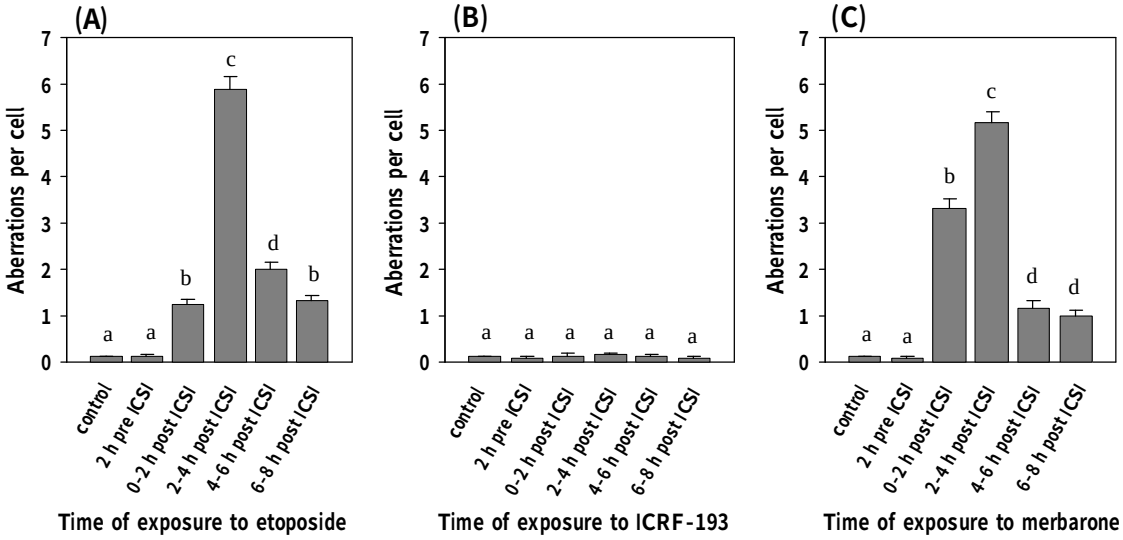
(A)
(B)
(C)
Aberrations per cell
0
1
2
3
4
5
6
7
a
a
b
c
d
b
a
a
a
a
a
a
a
a
b
c
d
d
control
2 h pre ICS
0-2 h post ICS
2-4 h post ICS
4-6 h post ICS
6-8 h post ICS
Time of exposure to etoposide
Time of exposure to ICRF-193
Time of exposure to merbarone

Figure 4

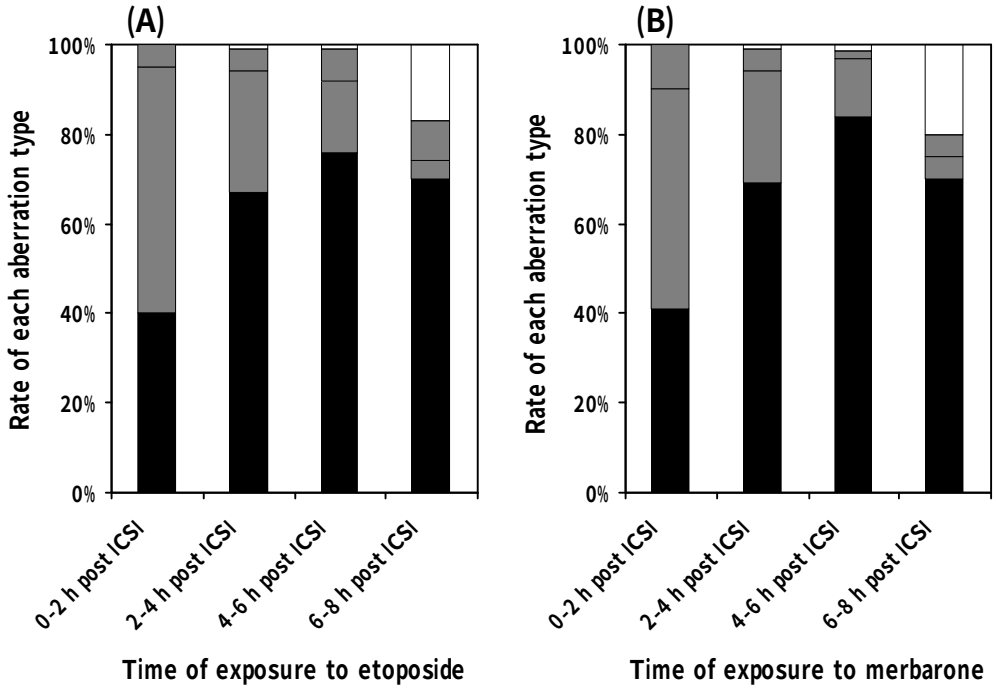
(A)
100%
80%
60%
40%
20%
0%
Rate of each aberration type
0-2 h post ICSI
2-4 h post ICSI
4-6 h post ICSI
6-8 h post ICSI
Time of exposure to etoposide
(B)
100%
80%
60%
40%
20%
0%
Rate of each aberration type
0-2 h post ICSI
2-4 h post ICSI
4-6 h post ICSI
6-8 h post ICSI
Time of exposure to merbarone